IWN 2014

WROCŁAW, POLAND
AUGUST 24-29, 2014

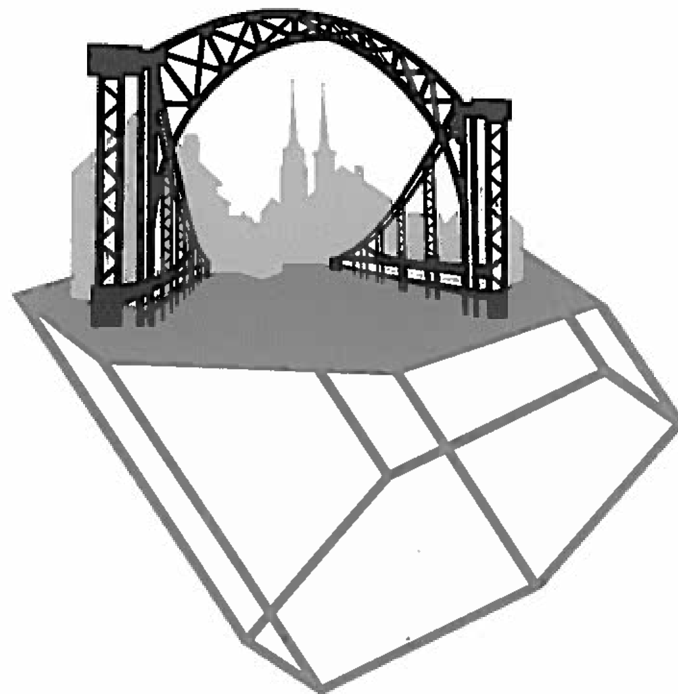

H.Yacoub(1), D.Fahle(1,2),M.Finken(1),C.Blumberg(3), W. Prost(3),H.Hahn(1), H.Kalisch(1), M.Heuken2and A.Vescan(1)

1.GaN Device Technology, RWTH Aachen University, Aachen, Germany
2.AIXTRON SE, Herzogenrath, Germany
3.Institute of Semiconductor Technology, Duisburg-Essen University, Germany

TuBP6

Effect of III-N Barrier Resistance on CV Characteristics in GaN-based MOSHEMTs in Spill-Over Regime.

M. Capriotti(1), P. Lagger(1,2), C. Fleury(1),R. Stradiotto(3),M. Oposich(1), C. Ostermaier(2),G. Strasser(1), D. Pogany(1)

1. Vienna University of Technology, Vienna, Austria
2. Infineon Technologies Austria AG, Villach, Austria
3. KAI GmbH, Villach, Austria

TuBP7

Type-II In0.17Al0.83N/GaN Band alignment: Experimental Evidence and Theoretical Interpretation.

J. M. Wang, F. J. Xua, W. An, X. Z. Li, J. Song, W. K. Ge, X. Q. Wang, N. Tang, Z. J. Yang and B. Shenb

State Key Laboratory of Artificial Microstructure and Mesoscopic Physics, School of Physics, Peking University, Beijing, China

TuBP8

Carrier dynamics in blue- and green-emitting InGaN/GaN quantum wells.

R. Aleksiejunas(1), K. Nomeika(1), S.Miasojedovas(1), S. Nargelas(1), P. Scajev(1), T.Malinauskas(1), M.Vengris(1), K. Jarasiunas(1), O. Tuna(2) and M. Heuken(2)

1. Vilnius university, Institute of Applied Research, Vilnius, Lithuania
2. AIXTRON SE, Herzogenrath, Germany

TuBP9

A Study of the Inclusion of Prelayers in InGaN/GaN Single and Multiple Quantum Well Structures.

Matthew J. Davies(1), Philip Dawson(1), Fabien C.-P. Massabuau(2), Rachel A. Oliver(2),Menno J. Kappers(2) and Colin J. Humphreys(2).

1. School of Physics and Astronomy, Photon Science Institute, University of Manchester, Manchester, M13 9PL, UK
2. Department of Materials Science and Metallurgy, University of Cambridge, Cambridge, UK

TuBP10

Correlation of Microstructure and Optical Properties of InGaN Quantum Wells on Metamorphic Buffer.

Christian Mounir(1), Jurgen Daubler(2), Thorsten Passow(2), Klaus Kohler(2),

Rolf Aidam(2), Michael Kunzer(2) and Ulrich T. Schwarz (1,2)

1. University of Freiburg, IMTEK, Freiburg, Germany
2. Fraunhofer Institute for Applied Solid State Physics, Freiburg, Germany

TuBP11

InGaN Quantum Wells on Semipolar Planes: Comparison of Growth and Optical Emission Properties on (20-21) and (20-2-1).

Ingrid L. Koslow(1), Nikolay Ledentsov(1), Monir Rychetsky(1), Martin Frentrup(1), Jens Rass(1), Tim Wernicke(1), Christian Mounir(2), Ulrich T. Schwarz(2), Ute Zeimer(3), Markus Weyers(3) and Michael Kneissl(1,3)

1. Technische Universitat Berlin, Institute of Solid State Physics, Berlin, Germany
2. Universitat Freiburg, IMTEK, Freiburg, Germany
3. Ferdinand-Braun-Institut, Leibniz-Institut fur Hochstfrequenztechnik, Berlin, Germany

TuBP12

Optical Studies of Non-Polar m-Plane (1-100) InGaN/GaN MQWs Grown on Freestanding Bulk GaN.

Danny Sutherland(1), Tongtong Zhu(2), Fengzai Tang(2), James T. Griffiths(2), Dmytro Kundys(1), Philip Dawson(1), Fabrice Oehler(2), Menno J. Kappers(2), Colin J. Humphreys(2), Rachel A. Oliver(2)

1. School of Physics and Astronomy, Photon Science Institute, University of Manchester, Manchester, UK
2. Department of Material Science and Metallurgy, University of Cambridge, Cambridge, UK

TuBP13

Importance of the dielectric contrast for the polarization of the photoluminescence of GaN nanowires.

Pierre Corfdir, Christian Hauswald, Johannes K. Zettler, Felix Feigentrager, Sergio Fernandez-Garrido, Manfred Ramsteiner, Lutz Geelhaar and Oliver Brandt

Paul-Drude-Institut fur Festkorperelektronik, Berlin, Germany

TuBP14

Luminescence Properties of Semipolar (11-22) InGaN Single Quantum Wells.

Duc V. Dinh(1), M. Hocker(2), T. Meyer(3), M. Caliebe(4), M. Pristovsek(5), K. Thonke(2), F. Scholz(4), C. J. Humphreys(5), P. J. Parbrook(1,6)

1. Tyndall National Institute, Cork, Ireland
2. Institute of Quantum Matter, Ulm University, Ulm, Germany
3. OSRAM Opto Semiconductors GmbH, Regensburg, Germany
4. Institute of Optoelectronics, Ulm University, Ulm, Germany
5. Department of Materials Science and Metallurgy, University of Cambridge, Cambridge, United Kingdom
6. School of Engineering, University College Cork, Ireland

Effect of III-N Barrier Resistance on CV Characteristics in GaN-based MOSHEMTs in Spill-Over Regime

M. Capriotti [1], P. Lagger [1,2], C. Fleury [1], R. Stradiotto [3], M. Oposich [1], C. Ostermaier [2], G. Strasser [1], D. Pogany [1]

[1] *Vienna University of Technology, Floragasse 7a, A-1040 Vienna, Austria*
[2] *Infineon Technologies Austria AG, Siemensstraße 2, A-9500 Villach, Austria*
[3] *KAI GmbH, Europastraße 8, A-9524 Villach, Austria*

Due to low gate leakage current and high gate voltage swing, GaN-based Metal Oxide Semiconductor High Electron Mobility Transistors (MOSHEMTs) are attractive for power electronic applications. However, they still suffer from threshold voltage (V_{th}) instability under forward bias conditions [1-4]. In the spill-over regime, where a second conductive channel is formed at the III-N/dielectric interface, the onset of the second capacitance rise is usually strongly frequency dependent [1]. It has recently been shown that the threshold voltage dynamics is governed not only by the capture and emission processes of traps at/near the dielectric/III-N interface but also by the effect of the conductance of the III-N barrier [2, 3]. Yang et al. also pointed out that the III-N barrier resistance can influence the extracted trap density using the conductance technique [4]. Therefore, they proposed to analyze the frequency and temperature dependence of the onset of the second rise in the CV curve for the trap density evaluation. In this paper, using a lumped element model with bias-dependent elements, we show that the frequency shift in the second capacitance rise can be solely explained by the effect of the barrier resistance, without considering the response of traps.

The heterostructure composed of 2 nm GaN cap layer, 25 nm $Al_{0.25}Ga_{0.75}N$, GaN channel and AlGaN nucleation layer was grown by MOCVD on highly doped silicon substrate. A 30nm SiO_2 layer was chemical vapor deposited on top of the heterostructure. Capacitor top electrode is composed by Pt/Au (area of 2000 μm^2). The CV analysis was performed with a Keithley 4100 using an equivalent parallel capacitance/conductance model. The voltage sweep was performed several times for each frequency, so that some typical quasi-stable hysteresis was observed in a group of curves. The group of curves is thus considered as typical and reproducible for this frequency.

The measured CV curve shows a typical shift in the second onset voltage, V_{so}, and a decrease of the second capacitance plateau with increasing frequency (Fig. 1). We simulate the CV curve (in general admittance) using a lumped element model in Fig. 2, considering that the capacitance increase at V_{so} is caused by the strong decrease in the barrier resistance R_{br} with increasing bias. This can be explained physically by the decrease of the barrier potential with increasing gate bias. This will gradually short-circuit the barrier capacitance leading to a capacitance increase, up to C_{ox}. The full model (Fig. 2), based on [5] includes: (i) the gradual decrease of the channel differential resistance R_c around V_{th}, which is related to inverse of transconductance of a HEMT device fabricated on the same structure, (ii) bias dependence of depletion capacitance C_d extracted from Fig.1 according to [5], (iii) gradual decrease of R_{br} from the region of $V < V_{so}$ to the region of $V > V_{so}$ where R_{br} saturates at a value consistent with the differential resistance of the bias-rescaled gate leakage current of a Schottky diode prepared on the same heterostructure. We point out again that in this model the response of traps is not included. The calculated capacitance and conductance curves according to this model (Fig.3) can explain all the main features of the experiments considering only the frequency dependent response of the equivalent circuit of Fig. 2. The shift in V_{so} is determined by the width of the transition region in R_{br} (see Fig.3c). The change in the capacitance plateau is due to finite value of R_{br} for $V > V_{so}$. In addition, the model